Supplementary Information for

Microfluidic-based in vitro thrombosis model for studying the microplastics toxicity

Longfei Chen,†[ab] Yajing Zheng,†[c] Yantong Liu,[ab] Pengfu Tian,[a] Le Yu,[a] Long Bai,[d] Fuling Zhou,[e] Yi Yang,[ab]* Yanxiang Cheng,[c]* Fubing Wang,[f] Li Zheng,[g] Fenghua Jiang,[g] Yimin Zhu,[d]

[a.]Key Laboratory of Artificial Micro- and Nano- Structures of Ministry of Education, School of Physics & technology, Wuhan University, Wuhan 430072, China.

[b.]Shenzhen Research Institute, Wuhan University, Shenzhen 518000, China.

[c.]Department of Obstetrics and Gynecology, Renmin Hospital of Wuhan University, Wuhan 430060, China

[d.]School of Medicine, Zhejiang University, Hangzhou, Zhejiang 310002, China.

[e.]Department of Hematology, Zhongnan Hospital, Wuhan University, Wuhan 430071, China.

[f.]Department of Laboratory Medicine, Zhongnan Hospital, Wuhan University, Wuhan 430071, China.

[g.]Institute of Oceanology, Chinese Academy of Sciences, Qingdao 266061, China.

Email: yangyiys@whu.edu.cn
yanxiangcheng@whu.edu.cn

This PDF file includes:

Figures S1 to S7

Supplementary Figures

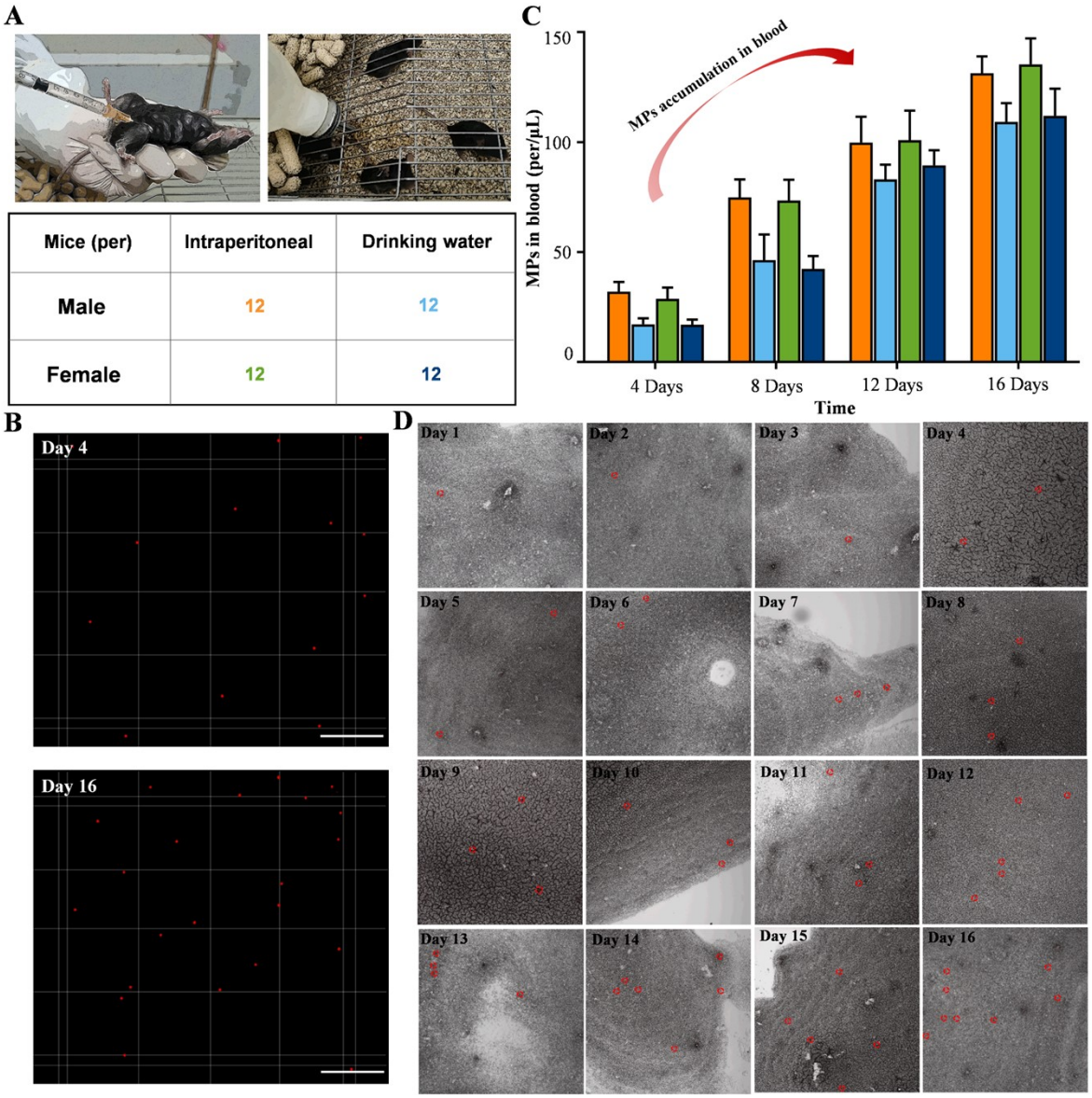

Fig. S1. The evaluation of MPs accumulation risk in vivo mice experiments. (a) Experimental design of micro-plastic peritoneal mucosal and intestinal transferring. (b) Confocal micrograph of counting MPs particles in blood. Scale bar: 250μm. (c) Histogram of accumulated MPs in four experimental groups. (d) Micrograph of MPs in blood with increasing time.

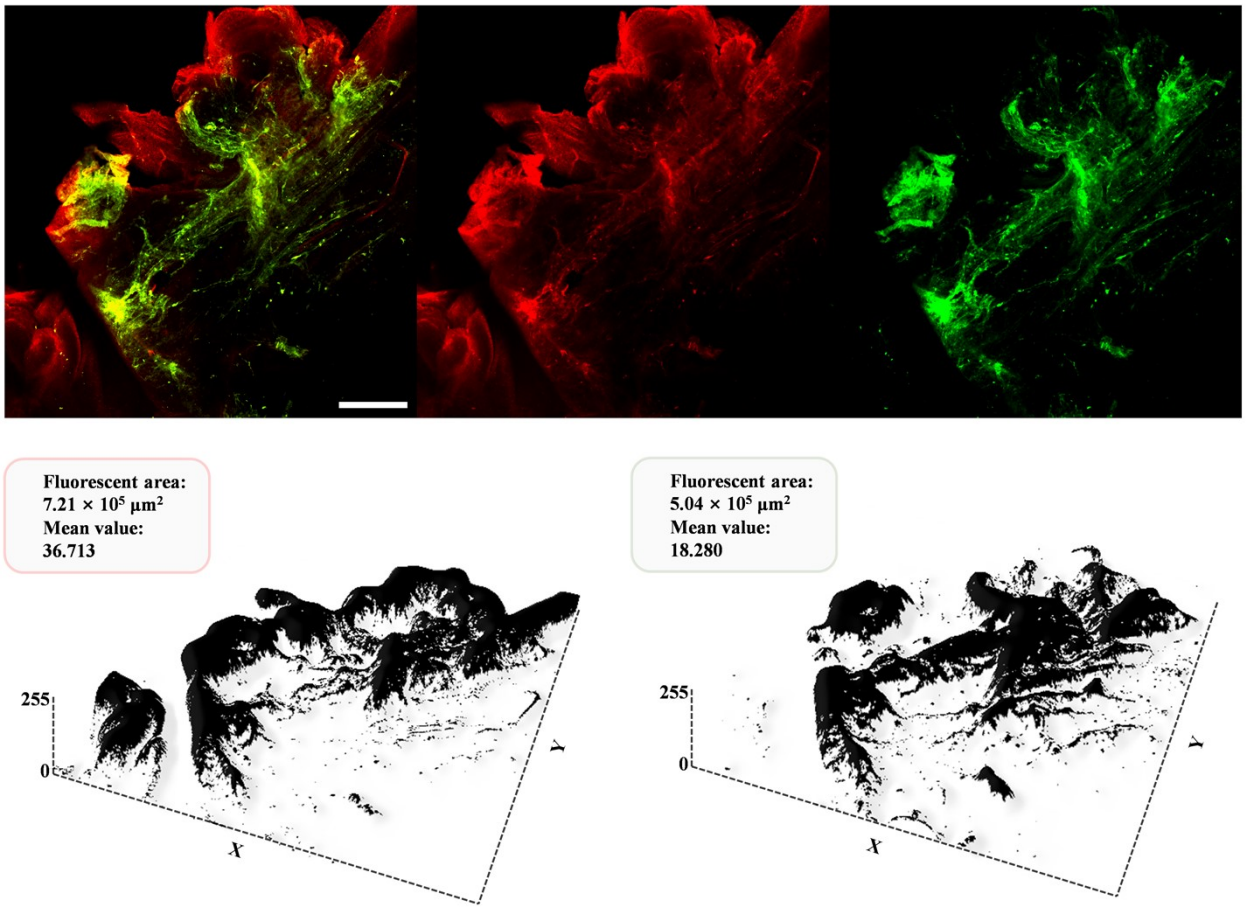

Fig. S2. The fluorescent analysis of normal thrombus. Laser confocal micrograph of normal thrombus, and 3D fluorescence intensity distribution map between PLT, FIB. Scale bar: 300μm.

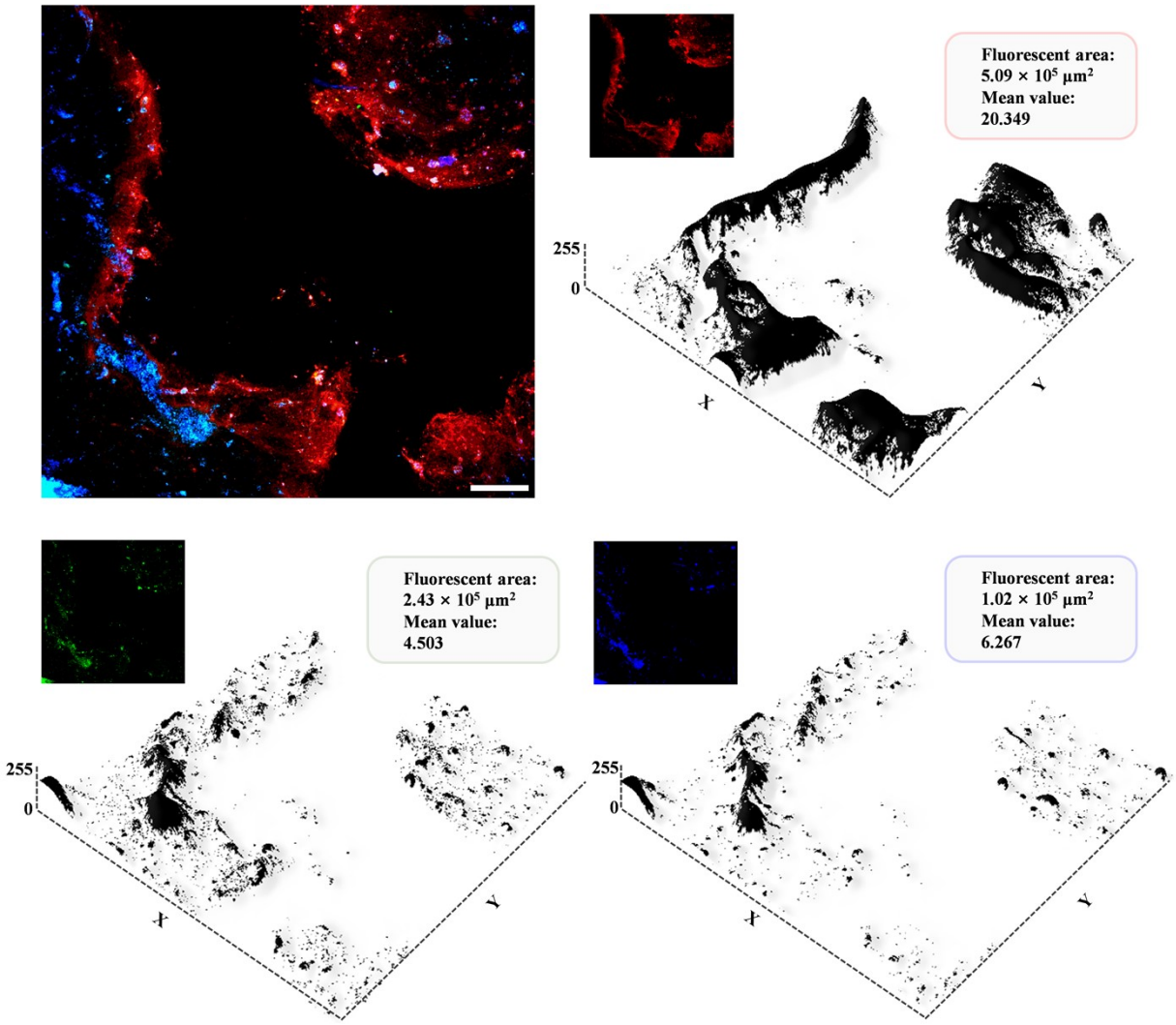

Fig. S3. The fluorescent analysis of MPs invasion. Laser confocal micrograph of MPs invasion, and 3D fluorescence intensity distribution map between PLT, FIB, MPs. Scale bar: 200μm.

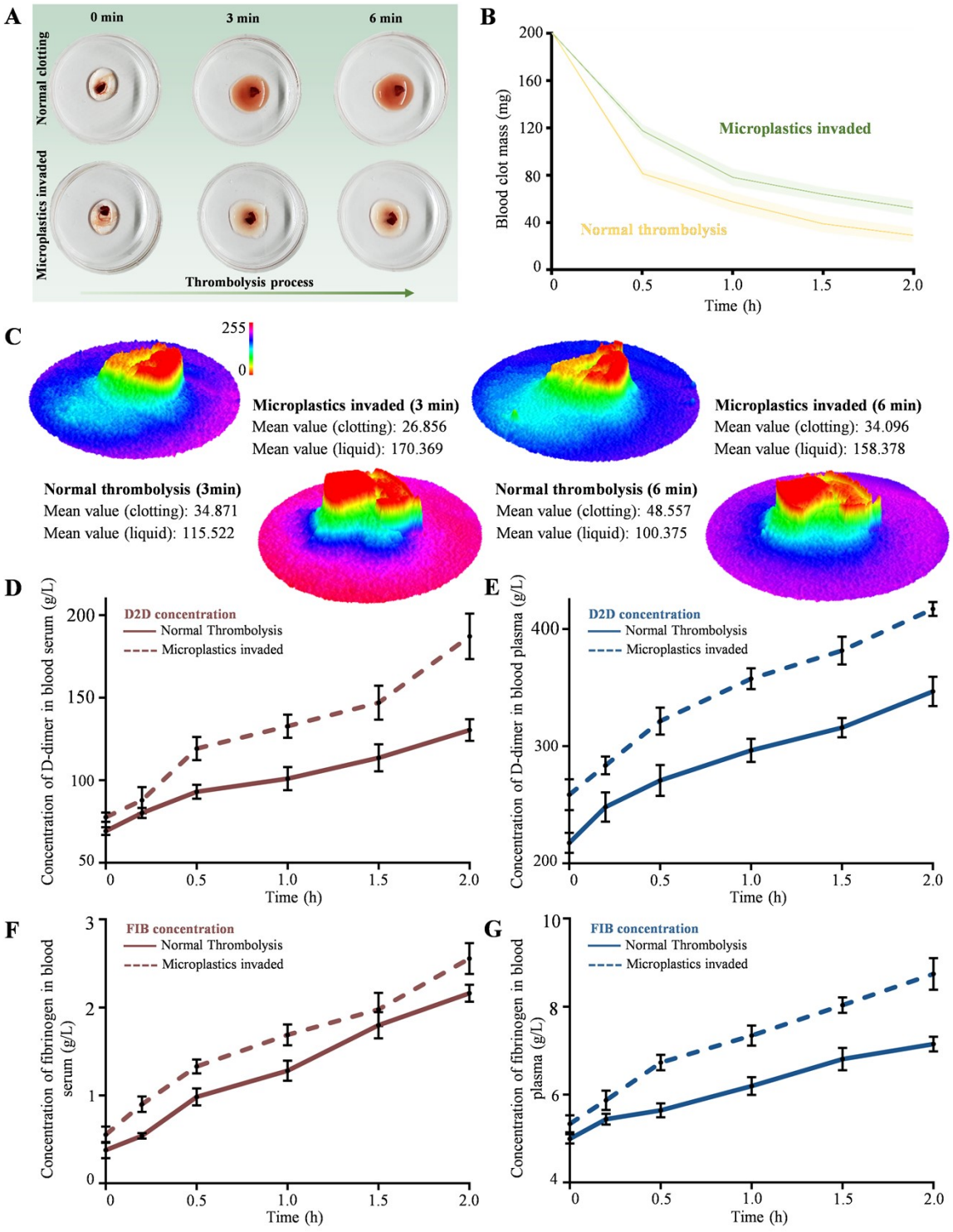

Fig. S4. The MPs effects on in-vitro thrombolysis and D-dimer, fibrinogen concentration analysis. (a) The in-vitro thrombolysis process of normal and MPs invasion. (b) The blood clotting mass of thrombolysis between normal and MPs invasion. (c) Three-dimensional light intensity distribution of normal thrombosis and MPs invasion. (d-e) The D-dimer concentration analysis between normal and MPs invasion (blood serum, blood plasma). (f-g) The fibrinogen concentration analysis between normal and MPs invasion (blood serum, blood plasma).

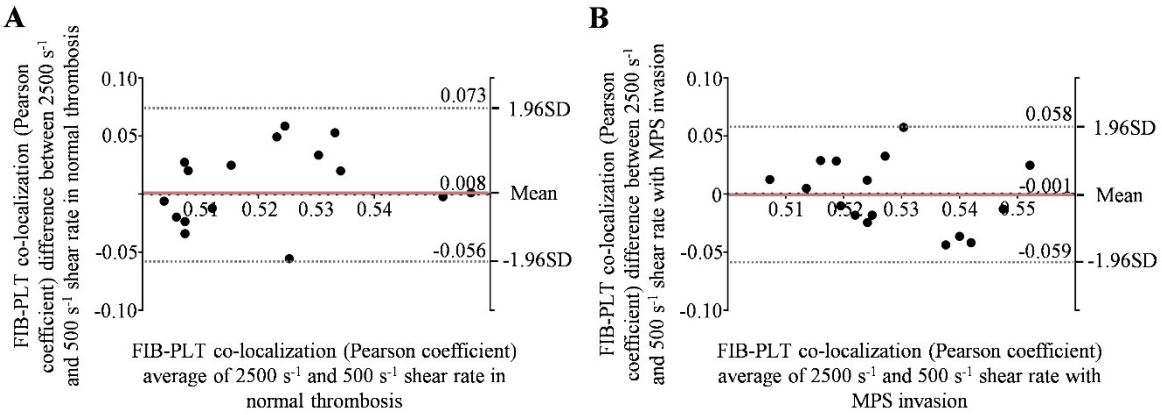

Fig. S5. The Bland–Altman analysis of FIB-PLT co-localization under different shear rate (normal, MPs invasion). (a) The Bland–Altman analysis to compare the FIB-PLT co-localization of normal thrombosis obtained by the 500 s^{-1} and 2500 s^{-1} shear rate. The red dashed line is the mean difference, and the gray dash lines represent the 95% LOAs. (b) The Bland–Altman analysis to compare the FIB-PLT co-localization of MPs invasion obtained by the 500 s^{-1} and 2500 s^{-1} shear rate.

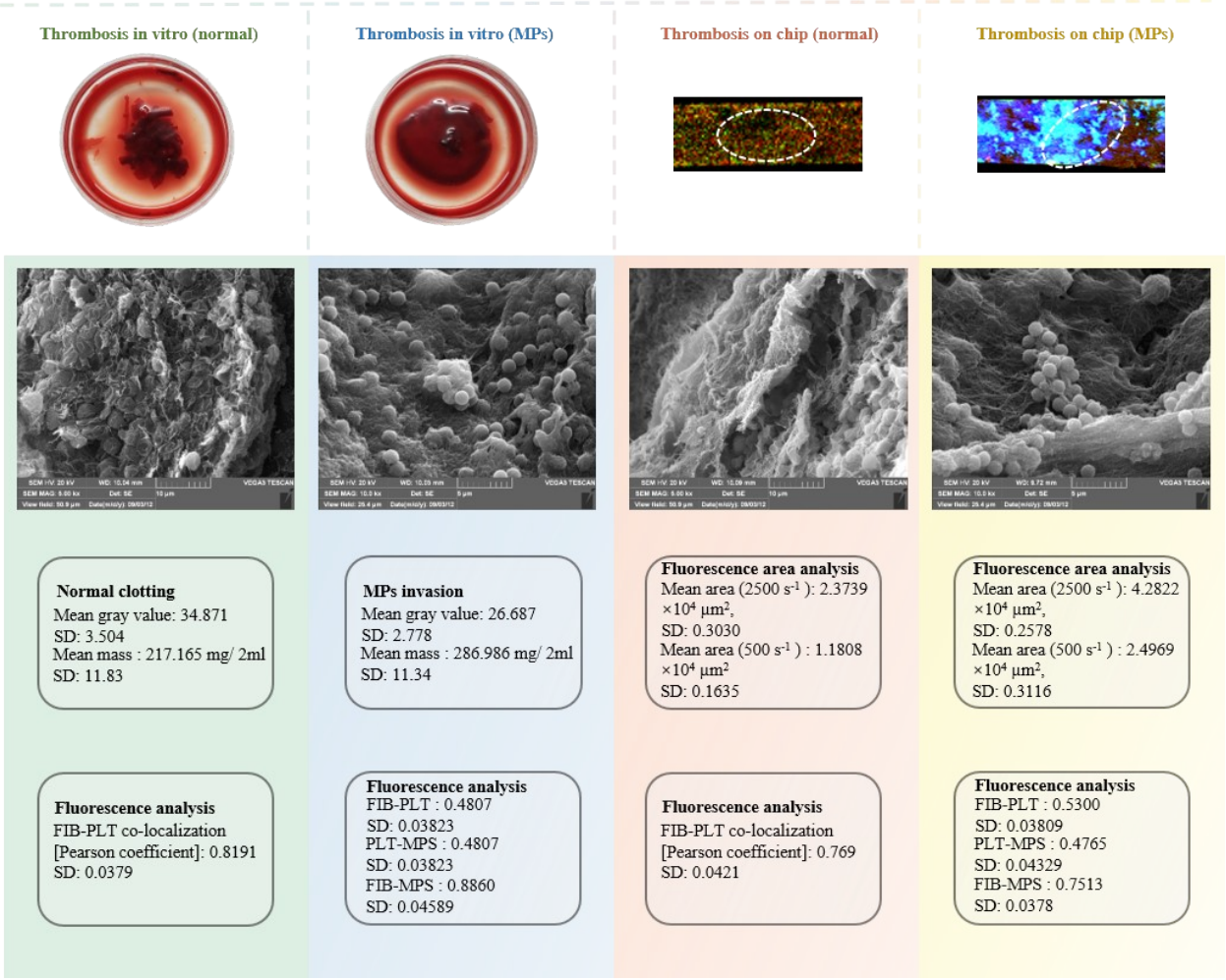

Fig. S6. The thrombus (mass, gray value, SEM, fluorescent area, fluorescent co-localization) analysis between thrombosis in vitro and on-chip.

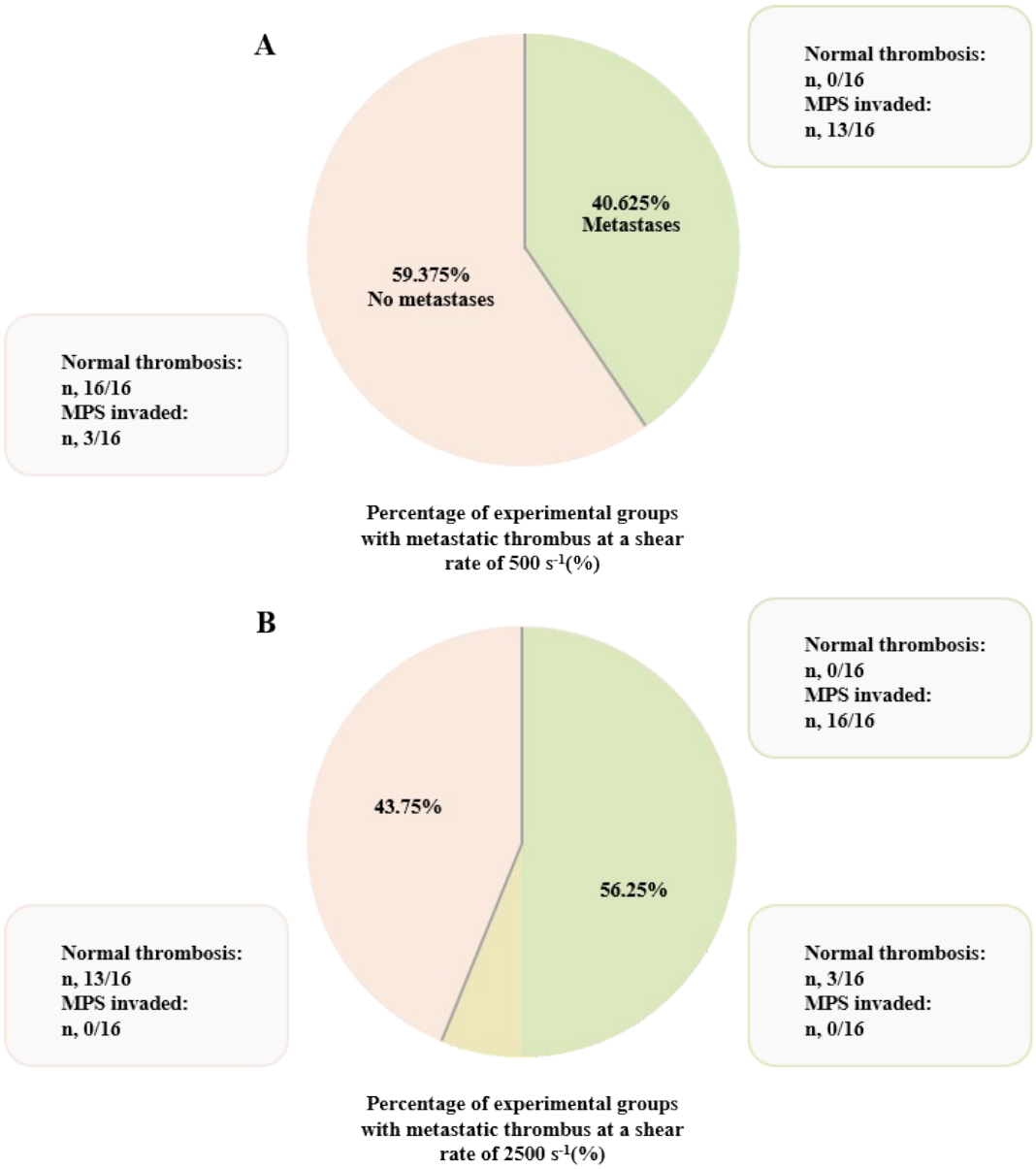

Fig. S7. The percentages of experimental groups accompanied by metastasis under different shear rate between normal thrombosis and MPs invasion.